Chronic low-dose dioxin exposure accelerates high fat diet-induced hyperglycemia in female mice

Geronimo Matteo[1]*, Myriam P Hoyeck[1]*, Hannah Blair[1], Julia Zebarth[1], Kayleigh RC Rick[1], Andrew Williams[2], Rene Gagné[2], Julie K Buick[2], Carole Yauk[2,3], Jennifer E Bruin[1#].

* Authors contributed equally

[1]Department of Biology & Institute of Biochemistry, Carleton University, Ottawa, Ontario, K1S 5B6 Canada.

[2] Environmental Health Science and Research Bureau, Health Canada, Ottawa, Ontario K1A 0K9 Canada.

[3]Department of Biology, University of Ottawa, Ontario, KIN 6N5

[#] Address correspondence to:
Dr. Jennifer Bruin
244 Nesbitt Biology Building
1125 Colonel By Drive
Ottawa, ON K1S 5B6
T: 613-520-2600 x3656
jenny.bruin@carleton.ca

Abstract:

Human studies consistently show an association between exposure to persistent organic pollutants, including 2,3,7,8-tetrachlorodibenzo-*p*-dioxin (TCDD, aka "dioxin"), and increased diabetes risk. We previously showed that acute high-dose (20 µg/kg) TCDD exposure decreased plasma insulin levels in both male and female mice *in vivo*, however effects on glucose homeostasis were sex-dependent. The current study investigated the impact of chronic low-dose TCDD exposure (20 ng/kg/d, 2x/week) on beta cell function and glucose homeostasis in male and female mice fed either a chow diet or high-fat diet (HFD) for 12 weeks. Low-dose TCDD exposure did not lead to adverse metabolic consequences in chow-fed male or female mice, or in HFD-fed males. However, TCDD accelerated the onset of HFD-induced hyperglycemia and impaired glucose-induced plasma insulin levels in female mice. In addition, islet RNAseq analysis showed that TCDD exposure promoted abnormal changes to endocrine and metabolic pathways in HFD-fed females. Our data supports a 'double-hit' hypothesis that TCDD exposure combined with HFD-feeding is more deleterious than either in isolation in female mice, and that chronic TCDD exposure increases diabetes susceptibility in females.

Keywords: dioxin, diabetes, sex differences, beta cells, insulin, hyperglycemia

Abbreviations

AhR	Aryl Hydrocarbon Receptor
CO	Corn oil
ELISA	Enzyme-linked immunofluorescence assay
GTT	Glucose tolerance test
GSIS	Glucose-stimulated insulin secretion
HFD	High-fat diet
ITT	Insulin tolerance test
PFA	Paraformaldehyde
POPs	Persistent organic pollutants
qPCR	Quantitative real-time PCR
TCDD	2,3,7,8-tetrachlorodibenzo-*p*-dioxin
T2D	Type 2 diabetes

Introduction

Global diabetes incidence is on the rise, yet the underlying cause for this increase remains to be elucidated (1). Genetics and lifestyle factors, such as physical inactivity and poor diet, are known risk factors for type 2 diabetes (T2D) (2,3). For example, high fat diet (HFD) feeding promotes hyperglycemia, hyperinsulinemia, and insulin resistance in both humans and rodents (4). However, these risk factors alone cannot account for the rapid increase in diabetes burden, but rather other environmental factors, such as environmental pollutants, may also be contributing.

Persistent organic pollutants (POPs) are of particular concern to human health since these compounds resist degradation and bioaccumulate in our environment. High serum POP concentrations are positively associated with a modest relative risk of developing T2D (5–10) and insulin resistance (11,12) both in populations exposed to high doses of pollutants (e.g. war veterans, victims of chemical disasters, and occupational workers) (13–15) and the general population exposed to chronic low-doses of pollutants (16–18). Most epidemiological studies investigating the association between POP exposure and diabetes risk only report data from males. Interestingly, the few studies that considered both males and females suggest that females may be at greater risk of developing diabetes following POP exposure. For example, follow up studies on the Seveso population exposed to 2,3,7,8-tetrachlorodibenzo-*p*-dioxin (TCDD, aka "dioxin") found a higher relative risk of developing diabetes in females than males (14,19). In addition, high serum PCB levels in the Michigan cohort (20) and Yucheng cohort (10) were associated with significantly increased diabetes incidence in women only. A causal link between POP exposure and T2D pathogenesis remains to be established and potential sex differences in pollutant-induced diabetes risk requires further investigation.

Dioxin/TCDD is a potent aryl hydrocarbon receptor (AhR) agonist and an excellent model chemical for investigating whether dioxin-like compounds increase diabetes risk. Although TCDD is now well regulated worldwide, there are hundreds of dioxin-like chemicals in our environment that remain a global concern for human health (21). We have shown that TCDD exposure induces AhR-regulated genes, including cytochrome P450 1a1 (*Cyp1a1*), in pancreatic islets *in vitro* and *in vivo*, demonstrating that TCDD reaches the endocrine pancreas (22). Direct TCDD exposure also significantly reduced glucose-stimulated insulin secretion in mouse and human islets *in vitro* (22). Interestingly, a single high-dose injection of TCDD (20 µg/kg) *in vivo* reduced plasma insulin levels in both male and female mice, but overall metabolic effects differed drastically between sexes (23). TCDD-exposed males had modest fasting hypoglycemia for ~4 weeks post-injection, increased insulin sensitivity, and decreased beta cell area compared to vehicle-exposed controls. Conversely, TCDD did not alter insulin sensitivity or islet composition in females, but did induce transient hyperglycemia during a glucose tolerance test (GTT) at 4 weeks post-injection (23). Whether similar sex-specific effects occur with a more physiologically relevant dose of TCDD remains to be investigated. However, we found that transient low-dose TCDD exposure during pregnancy/lactation in female mice did not impact glucose homeostasis in chow-fed mice, but promoted HFD-induced obesity and hyperglycemia post-exposure (24). These results suggest that chronic low-dose TCDD exposure on its own may not cause diabetes but may increase diabetes susceptibility when challenged with a secondary metabolic stressor, such as HFD feeding. Whether this is specific to female mice or also occurs in males, remains to be determined.

The effects of concurrent TCDD exposure and HFD feeding, termed a 'double-hit', are not well understood. One study showed that TCDD exposure promoted hepatic fatty acid deposition in HFD fed female mice (25). In addition, intestinal and hepatic lipid transport genes were significantly upregulated in chow-fed female mice exposed to TCDD compared to vehicle controls, suggesting that TCDD exposure increases hepatic lipid storage, a hallmark of insulin resistance (25). These data support that a 'double-hit' of concurrent TCDD exposure and HFD-feeding is more deleterious than either alone in hepatic tissue. However, the potential impact on systemic glucose homeostasis and the endocrine pancreas have not been reported. The purpose of this study was to determine whether chronic-low dose TCDD exposure impairs beta cell function and/or glucose homeostasis in a sex-dependent manner in either chow-fed or HFD-fed mice.

Methods

Animals

Male and female C57BL/6 mice, 6-8 weeks old (Charles River; Raleigh, NC, USA), were maintained on a 12-hour light/dark cycle. All mice received *ad libitum* access to a standard chow diet for 1 week prior to starting experimental treatments. All experiments were approved by Carleton University and University of Ottawa Animal Care Committees and carried out in accordance with Canadian Council on Animal Care guidelines. All experimental groups were matched for mean body weight and fasting blood glucose levels prior to starting treatments to ensure that the groups were not significantly different.

As outlined in **Fig. 1A**, male and female mice received intraperitoneal (i.p.) injections of CO (vehicle control, 25 ml/kg) (#48599, Sigma Aldrich, St. Louis, MO, USA) or a low-dose of TCDD (20 ng/kg/d) (Sigma Aldrich, # 48599) 2x/week for 12 weeks. Simultaneously, mice were fed either standard rodent chow (20% fat, 66% carbohydrate, 14% protein; #2918, Harlan Laboratories, Madison, WI, USA) or a HFD (45% fat, 35% carbohydrate, 20% protein; #D12451, Cedarlane, Burlington, ON, Canada), generating the following experimental groups (n=10 per group per sex): COChow, COHFD, TCDDChow, TCDDHFD. Whole pancreas was isolated from a subset of mice at week 12 of the study and stored in 4% paraformaldehyde (PFA; #AAJ19943K2, Thermo Fisher Scientific, Waltham, MA, USA) for 24 hrs, followed by long-term storage in 70% EtOH for histological analysis (n=4-5 per group per sex). Pancreatic islets were isolated from a different subset of female mice at week 12 and stored in RNAlater (#76106, Qiagen, Hilden, Germany) for analysis by quantitative real-time PCR (qPCR) and RNAseq (n= 3-5 per group per sex).

Metabolic Assessments

All metabolic assessments were performed on conscious, restrained mice. Blood samples were collected via the saphenous vein using heparinized microhematocrit tubes at the indicated time points and measurements were performed using a handheld glucometer (Johnson & Johnson, New Brunswick, NJ, USA).

Body weight and blood glucose measurements were performed weekly following a 4-hour morning fast. For all metabolic assessments, time 0 indicates the blood collected prior to glucose or insulin administration. For GTTs, mice received an i.p. bolus of glucose (2 g/kg) following a

4-hour fast. Blood samples were collected at 0, 15, and 30 minutes for measuring plasma insulin levels by ELISA (#80-INSMSU-E01, ALPCO, Salem, NH, USA). For insulin tolerance tests (ITT), mice received an i.p. bolus of insulin (0.7 IU/kg, #02024233, Novo Nordisk, Toronto, Canada) following a 4-hour morning fast. Mice from different treatment groups were randomly distributed throughout all experiments to ensure that timing of blood collection did not affect our analysis.

Immunofluorescence staining and image quantification

Tissues were processed and embedded in paraffin wax blocks (University of Ottawa Heart Institute, Ottawa, ON, Canada) and then sectioned into 5 µm slices (Thermo Scientific Microm HM 3558). Immunofluorescence staining was performed as previously described (22). In brief, slides were deparaffinized with sequential incubations in xylene and ethanol. Heat-induced epitope retrieval was performed in 10 mM citrate buffer at 95°C for 10-15 minutes, and slides were incubated with Dako Serum Free Protein Block (#X090930-2, Agilent, Santa Clara, CA, USA) for 30 minutes at room temperature. Slides were incubated overnight at 4°C with primary antibodies, and then incubated with secondary antibodies for 1-hour at room temperature. Coverslips were mounted with Vectashield® hardset mounting medium with DAPI (#H-1500, Vector Laboratories, Burlingame, CA, USA).

The following primary antibodies were used: rabbit anti-insulin (1:200, C27C9, #3014, Cell Signaling Technology), and mouse anti-glucagon (1:1000; #G2654, Sigma Aldrich). The following secondary antibodies were used: goat anti-mouse IgG (H+L) secondary antibody, Alexa Fluor 488 (1:1000, Invitrogen, #A11029); and goat anti-rabbit IgG (H+L) secondary antibody, Alexa Fluor 594 (1:1000, Invitrogen, #A11037).

Whole pancreas sections were imaged using a Zeiss Axio Observer 7 microscope, and immunofluorescence was manually quantified using Zen Blue 2.6 software (Zeiss, Oberkochen, Germany). For all measurements, a range of 4-36 islets per mouse were quantified and the average was reported for each biological replicate. The % hormone$^+$ area per islet was calculated as [(hormone$^+$ area / islet area) x 100].

Islet Isolation

Islets were isolated by pancreatic duct injections with collagenase (1000 U/ml; #C7657, Sigma-Aldrich) as previously described (22). In brief, inflated pancreas tissues were excised and incubated at 37°C for 12 min, and the collagenase reaction quenched with cold Hank's balanced salt solution (HBSS) with 1mM $CaCl_2$. The pancreas tissue was washed in HBSS+$CaCl_2$ and resuspended in Ham's F-10 (#SH30025.01, HyClone, GE Healthcare Bio-sciences, Pittsburgh, PA, USA). Pancreas tissue was filtered through a 70 µm cell strainer and islets were handpicked under a dissecting scope to >95% purity.

Quantitative Real Time PCR

RNA was isolated from pancreatic islets using the RNeasy Micro Kit (#74004, Qiagen) as per the manufacturer's instructions, with the following amendment: 7 volumes of buffer RLT + DTT were added to the samples prior to lysing with 70% EtOH. DNase treatment was performed prior to cDNA synthesis with the iScript^{TM} gDNA Clear cDNA Synthesis Kit (#1725035, Biorad, Mississauga, ON, Canada). qPCR was performed using SsoAdvanced Universal SYBR Green

Supermix (Biorad, #1725271) and run on a CFX96 or CFX394 (Biorad). *Ppia* was used as the reference gene since it displayed stable expression under control and treatment conditions. Data were analyzed using the $2^{\Delta\Delta CT}$ relative quantitation method. Primer sequences are listed in **Supp. Table 1**.

Tempo-Seq®

Gene expression in whole islets was measured using the TempO-Seq Mouse Whole Transcriptome panel (BioSpyder Technologies Inc, Carlsbad, CA). 2 µl of RNA was diluted in 2x TempO-Seq lysis buffer diluted with an equal amount of PBS. Lysates, positive controls (100 ng/µl of Universal Mouse Reference RNA (UMRR) Quantitative PCR Mouse Reference Total RNA Agilent, cat # 750600), and no-cell negative controls (1X TempO-Seq lysis buffer alone) were hybridized to the detector oligo mix following the manufacturer's instructions (TEMPO-SEQ Mouse Mouse Whole Transcriptome AssayTranscriptome Kit (96 Samples) BioSpyder Technologies, Inc. Carlsbad, CA, USA). Hybridization was followed by nuclease digestion of excess oligos, detector oligo ligation, and amplification of the product with the tagged primers according to manufacturer's instructions. Each sample's primers were also ligated to a sample-specific barcode that allows multiplexing for sequencing purposes. Labelled amplicons were pooled and purified using NucleoSpin Gel and PCR Clean-up kits (Takara Bio USA, Inc, Mountain View, CA USA). Libraries were sequenced in-house using a NextSeq 500 High-Throughput Sequencing System (Illumina, San Diego, CA, USA) using 50 cycles from a 75-cycle high throughput flow cell. A median read depth of 2 million reads/sample was achieved.

Reads were extracted from the bcl files, demultiplexed (i.e., assigned to respective sample files) and were processed into fastq files with bcl2fastq v.2.17.1.14. The fastq files were processed with the "pete. star. script_v3.0" supplied by BioSpyder. Briefly, the script uses star v.2.5 to align the reads and the qCount function from QuasR to extract the feature counts specified in a gtf file from the aligned reads. The data were then passed through internal quality control scripts. Boxplots of the log2 CPM (counts per million) were plotted to ensure a reproducible distribution between replicates within a group. Hierarchical clustering plots were generated (hclust function: default linkage function of hclust function in R; complete-linkage) using a distance metric defined as 1-Spearman correlation in order to identify potential outliers. Probes with low counts (i.e. less than a median of 5 counts in at least one group) were flagged as absent genes and eliminated from the dataset. DEG analysis was conducted using the R software (26) on the counts using the default parameters of DESeq2 (27) with respective control and exposure groups. A shrinkage estimator was applied to the fold change estimates using the apeglm method (28) using the lfcShrink() function.

Probes reaching the threshold of an adjusted p-value < 0.05 and an absolute fold change > 1.5 (on a linear scale) were defined as differentially expressed genes (DEGs) and were retained for pathway analysis. Gene set analysis using KEGG pathways was conducted using DAVID (29,30). Pathways with a modified Fisher Extract p-value < 0.05 were considered enriched. Data are presented as bar graphs showing pathway fold enrichment, and secondly, as bar graphs with DEG counts for pathways that were trending ($p = 0.05 - 0.1$) or significantly enriched ($p < 0.05$). Pathways that were not trending or significantly enriched are indicated on bar graphs as not having the DEG count minimum threshold for significance.

Statistical analysis

Statistical analysis was performed using GraphPad Prism Software (GraphPad Software Inc., La Jolla, CA). Specific statistical tests are indicated in the figure legends and $p<0.05$ was considered statistically significant for all analyses. Statistically significant outliers were detected by a Grubbs' test with $\alpha=0.05$. All data was tested for normality using a Shapiro-Wilk test and for equal variance using either a Brown-Forsyth test (for one-way ANOVAs) or an F test (for unpaired t tests). Non-parametric statistics were used in cases where the data failed normality or equal variance tests. Parametric tests were used for all two-way ANOVAs, but normality and equal variance were tested on area under the curve values and by one-way ANOVAs. Data in line graphs are presented as mean ± SEM. Data in box and whisker plots are displayed as median, with whiskers representing maximum and minimum values. Each individual data point represents a different biological replicate (i.e. individual mouse).

Data and resource availability

The datasets generated and/or analyzed during the current study are available from the corresponding author upon reasonable request. Raw RNAseq data have been submitted to GEO (GEO: GSE144765).

Results

Chronic low-dose TCDD exposure does not impact body weight or fasting blood glucose levels in chow-fed or HFD-fed mice

Male and female mice were exposed to CO (vehicle) or 20 ng/kg/d TCDD 2x/week for 12 weeks, and simultaneously fed either a chow diet or 45% HFD (**Fig. 1A**). We were particularly interested in whether chronic low-dose TCDD exposure alone would promote weight gain (i.e. COChow vs TCDDChow) and/or accelerate diet-induced obesity (i.e. COHFD vs TCDDHFD) as previously seen in female mice exposed to TCDD during pregnancy (24). Interestingly, TCDD exposure had no effect on body weight in chow-fed females in this study (**Fig. 1B**). In addition, female mice were resistant to HFD-induced weight gain within the 12-week study timeframe, regardless of chemical treatment (**Fig. 1B**). Likewise, TCDD exposure did not alter body weight in chow-fed or HFD-fed male mice, but HFD feeding promoted significant weight gain compared to chow feeding in male mice from days 73 to 86 (**Fig. 1C**). TCDD exposure did not influence fasting blood glucose levels in any group, but HFD feeding caused fasting hyperglycemia in both CO- and TCDD-exposed females (**Fig. 1D,E**) and males (**Fig. 1F,G**).

TCDD exposure accelerates the onset of HFD-induced hyperglycemia in female mice

TCDD had no effect on glucose tolerance in chow-fed female or male mice at weeks 4 and 8 of the study (COChow vs TCDDChow; **Fig. 2i**). However, we observed an interaction between TCDD exposure and HFD feeding in female mice (**Fig. 2i**). At week 4, HFD feeding had no impact on glucose tolerance in CO-exposed females (COChow vs COHFD; **Fig. 2Aii,2B**), but TCDDHFD females were significantly hyperglycemic at 15- and 30-minutes post-glucose bolus and had a significantly elevated overall glucose excursion compared to TCDDChow females (TCDDChow vs TCDDHFD; **Fig. 2Aiii,2B**). By week 8, both COHFD and TCDDHFD females were glucose intolerant compared to chow-fed females (**Fig. 2C,D**). In contrast, HFD-fed male mice were significantly hyperglycemic following a glucose stimulus after 4 and 8 weeks of exposure compared to chow-fed males, irrespective of chemical exposure (**Fig. 2E-H**). In other words, both TCDD-exposed and CO-exposed males showed a similar response to HFD feeding

(**Fig. 2E-H**), whereas HFD-fed female mice had accelerated onset of hyperglycemia in the presence of TCDD (**Fig. 2A-D**).

TCDD-exposed female mice lack a compensatory hyperinsulinemic response to HFD feeding but show normal insulin tolerance

We next assessed whether TCDD altered circulating insulin levels during a GTT. After 8 weeks of HFD feeding, COHFD females showed an expected compensatory increase in plasma insulin levels during the GTT (**Fig. 3A**), ~2.3-fold more insulin overall than COChow females (**Fig. 3A-AUC**). In contrast, TCDDHFD females did not show the same compensatory response, and instead plasma insulin levels during the GTT were comparable to chow-fed females (**Fig. 3A**). TCDD did not impact insulin levels in either chow-fed or HFD-fed male mice (**Fig. 3B**), but rather diet had an overall effect on insulin levels in males (**Fig. 3B**, $p_{diet}<0.01$). These results suggest that TCDD exposure may cause abnormal insulin secretion in HFD-fed females only.

To determine whether the accelerated hyperglycemia in TCDDHFD female mice was driven in part by changes in peripheral insulin sensitivity, we performed ITTs at weeks 5 and 9. HFD-fed male and female mice were not overtly insulin resistant in this study (**Fig. 3C-F**). At week 5, COHFD females were slightly more insulin sensitive than COChow females at 60 minutes after the insulin bolus (**Fig. 4C**), and at week 9 TCDDChow females were modestly insulin sensitive at 15 minutes post bolus compared to COChow females (**Fig. 4E**), but otherwise there were no overall changes in blood glucose levels during ITTs, as measured by area under the curve (**Fig. 3C-F**).

We also measured expression of genes involved in insulin-dependent lipogenesis and gluconeogenesis pathways in the liver at week 12 as another indicator of insulin sensitivity. In females, HFD feeding significantly downregulated genes involved in gluconeogenesis (**Supp. Fig. 1A**, $p_{diet}<0.05$), including *G6pc* (glucose-6-phosphatase catalytic subunit), *Ppargc1a (*peroxisome proliferator-activated receptor gamma coactivator 1 alpha), and *Pck1* (phosphoenolpyruvate carboxykinase 1). There was a significant interaction between TCDD and HFD exposure on expression of *Acacb* (acetyl-CoA carboxylase beta; **Supp. Fig. 1A**, $p_{interaction}<0.05$), but this was modest and unlikely to explain the differences observed in plasma insulin levels or glucose homeostasis in female mice. There were no differences in any of the measured genes in the liver of male mice following TCDD and/or HFD exposure (**Supp. Fig. 1B**).

Islet size and endocrine composition were unchanged by TCDD exposure

To investigate why TCDD-exposed female mice did not develop hyperinsulinemia following HFD feeding, we examined islet size and endocrine cell composition. We predicted that HFD-fed mice might show increased islet size compared to chow-fed mice, but this was not the case in either male or female mice (**Fig. 4A,D**). Surprisingly, there was a significant overall effect of TCDD exposure to increase average islet size in male mice (**Fig. 4D**, $p_{chemical}<0.05$). We did not observe any changes in the % of islet area that was immunoreactive for either insulin (**Fig. 4B, E,G**) or glucagon (**Fig. 4C,F,G**) in either sex.

TCDDHFD female mice have enriched endocrine-related pathways in islets relative to COChow females

Since our histological findings did not explain the phenotype observed in TCDDHFD females, we performed RNAseq analysis on isolated islets from a subset of females at week 12 of the study to assess whole transcriptomic changes. We first compared all experimental groups to COChow females to investigate the effect of TCDD or HFD feeding alone (i.e. TCDDChow and COHFD, respectively), and in combination (TCDDHFD). TCDDChow females had 956 differentially expressed genes (DEGs), whereas COHFD females had 2121 DEGs and TCDDHFD females had 2667 DEGs compared to COChow females (**Fig. 5A**). Interestingly, only 50 DEGs were uniquely common between TCDDChow and TCDDHFD females, and only 196 were unique to TCDDChow (**Fig. 5A**). These results suggest that TCDD alone has very minor effects on gene expression in whole islets, which supports our *in vivo* observations (**Figs. 1-4**). Furthermore, 893 DEGs were uniquely common between HFD groups; 1180 DEGs were unique to TCDDHFD females and 518 DEGs unique to COHFD females (**Fig. 5A**), suggesting that TCDD may be driving abnormal changes in gene expression in response to HFD feeding.

Next, we performed KEGG pathway analysis on DEGs in **Fig. 5A** (TCDDChow, COHFD, and TCDDHFD females were each compared to COChow) using DAVID. Since pathway enrichment is determined based on total number of DEGs and the number of DEGs varied between our experimental groups (**Fig. 5A**), we presented pathway analysis as both pathway fold enrichment and number of DEGs within each pathway to avoid misinterpretation of our results. We first assessed pathways that were uniquely enriched in TCDDChow females to determine the effects of TCDD alone on the islet transcriptome (**Fig. 5Bi**). As expected, "Xenobiotic Metabolism by CYP450" was highly enriched in TCDDChow compared to COChow females, and 50% of the pathways enriched in TCDDChow females were involved in drug/chemical exposure, suggesting that TCDD alone mainly alters drug metabolism in islets. It is important to note that although "Xenobiotic Metabolism by CYP450" was not significantly enriched in COHFD or TCDDHFD females, a greater number of genes in the pathway were altered in HFD-fed than chow-fed females (**Fig. 5Bi**), suggesting that both TCDD exposure and HFD feeding alter this pathway.

We also assessed pathways that were enriched in COHFD and TCDDHFD females compared to COChow controls to identify transcriptomic differences that may explain why TCDDHFD females lacked a compensatory increase in insulin secretion (**Fig. 3A**). "Maturity Onset Diabetes of the Young" (MODY) was the most enriched pathway in COHFD compared to COChow females, but the number of DEGs was similar in both HFD groups irrespective of chemical treatment (**Fig. 5Bii**). In addition, "Insulin Secretion" was enriched in both HFD groups, although more genes were altered in TCDDHFD females compared to COHFD females (**Fig. 5Biv**). Interestingly, several pathways involved in beta cell function were differentially enriched in COHFD and TCDDHFD females. First, "Regulation of Actin Cytoskeleton" was significantly altered in COHFD females but not TCDDHFD females, with 35 DEGs in COHFD females (**Fig. 5Bii**). Therefore, changes in the actin cytoskeleton in islets may be a normal response to HFD feeding that is absent in the TCDDHFD condition. Second, "Circadian Rhythm" was the most enriched pathway in TCDDHFD compared to COChow females, and more genes within this pathway were changed in TCDDHFD females compared to COHFD females (**Fig. 5Bv**). Likewise, "FoxO1 Signaling Pathway" was enriched in TCDDHFD females, and more genes were altered in this pathway in TCDDHFD females compared to COHFD females (**Fig. 5Bv**). Lastly, thyroid hormone signaling pathway was significantly altered in TCDDHFD females only (**Fig. 5Bv**).

TCDDHFD females have inappropriate Cyp1a1 and circadian rhythm gene expression
To better understand the effect of TCDD exposure on the islet transcriptome, we generated both hierarchical heatmaps (**Fig. 6**) and heatmaps organized by experimental group (**Supp. Fig. 2**) for pathways of interest that were enriched in TCDDChow and TCDDHFD females compared to COChow controls (**Fig. 5**). We were particularly interested in the "Xenobiotic Metabolism by CYP450" pathway since we have previously shown that TCDD induces CYP1A1 enzymes in islets (22,23). We expected to see distinct clustering between CO- and TCDD-exposed females, but instead TCDD-exposed and COHFD females had a similar gene expression profile compared to COChow females (**Fig. 6A, Supp. Fig. 2A**). However, TCDDChow females formed a sub-cluster, indicating slight differences in gene expression compared to HFD-fed females (**Fig. 6A**). We further assessed the effect of TCDD on xenobiotic metabolism by specifically looking at *Cyp1a1* expression as a marker of AhR activation by dioxin exposure (22,23). Interestingly, *Cyp1a1* was upregulated ~3.5-fold and ~3.2-fold in TCDDChow and COHFD females, respectively, compared to COChow females (**Fig. 6C**). In contrast, TCDDHFD islets showed a non-significant trend towards having only ~2-fold higher *Cyp1a1* expression compared to COChow females, and *Cyp1a1* levels remained significantly lower than in TCDDChow females (**Fig. 6C**). These results suggest that crosstalk between TCDD exposure and HFD feeding prevents normal *Cyp1a1* induction in islets. These findings were validated by qPCR (**Fig. 6D**).

We also assessed circadian rhythm gene expression patterns since this pathway was the most enriched in TCDDHFD females (**Fig. 5Bv**). As expected, changes in circadian rhythm gene expression were mainly driven by diet, with chow-fed and HFD-fed females forming two distinct clusters (**Fig. 6B**). However, within both diet clusters we observed subclusters that were driven by chemical exposure (**Fig. 6B, Supp. Fig 2B**), suggesting that TCDD may be altering circadian rhythm in islets.

Chronic low-dose TCDD exposure promotes diet-induced changes in amino acid metabolism
Our *in vivo* results (**Figs. 2-3**) and previous findings from a separate study in pregnant mice (24) suggest that in females, background exposure to TCDD accelerates HFD-induced changes in metabolism. As such, we next investigated the effects of HFD feeding on the islet transcriptome of females with either CO or TCDD background exposure (i.e. COHFD vs COChow compared to TCDDHFD vs TCDDChow). Interestingly, COHFD females had 1674 unique DEGs relative to COChow females, whereas TCDDHFD had 706 unique DEGs relative to TCDDChow females (**Fig. 7A**), indicating that the effect of HFD varies depending on chemical exposure. In fact, KEGG pathway analysis revealed significant differences between COHFD and TCDDHFD females when compared to their respective chow-fed controls (**Fig. 7B**). As with our findings in **Fig. 5B**, MODY was the most enriched pathway in COHFD females; this pathway was also altered in TCDDHFD females but to a lesser extent (**Fig. 7Bi**). "Regulation of Actin Cytoskeleton" and "PI3K-Akt Signaling Pathway" were only altered by HFD feeding when mice were on a CO background (**Fig. 7Bi**), suggesting that TCDD exposure may prevent these normal responses to HFD feeding. Most interestingly, the top two most enriched pathways in TCDDHFD compared to TCDDChow females were "Alanine, Aspartate & Glutamate metabolism", and "Tyrosine Metabolism" (**Fig. 7Bii**). In fact, 40% of significantly enriched pathways in TCDDHFD females are involved in amino acid metabolism (**Fig. 7Bii**), suggesting

that background exposure to TCDD may promote abnormal changes to amino acid metabolism in HFD-fed females.

HFD-induced changes in MODY genes and Alanine, Aspartate, and Glutamate metabolism are promoted by TCDD exposure.

We generated heatmaps of the most enriched pathway in COHFD and TCDDHFD females with respect to their chow-fed controls (**Fig. 7B**). Interestingly, the "MODY" heatmap showed that TCDDHFD females formed a unique cluster compared to all other groups (**Fig. 8A, Supp. Fig. 2C**), suggesting an interactive effect of HFD feeding and TCDD exposure on expression of islet-specific genes. We next looked at specific genes essential for maintaining beta cell function and found a distinct pattern of gene expression in TCDDHFD females compared to COHFD females (**Fig. 8A, 8C-H, Supp. Fig. 2C**). Expression of *MafA* and *Slc2a2* were significantly downregulated in TCDDHFD females compared to COChow and TCDDChow females, whereas expression was only trending towards being downregulated in COHFD females (**Fig. 8C, D, H**). Similarly, *Hnf4α* was downregulated by HFD feeding, but this effect was worsened in TCDD-exposed females (**Fig. 8G**), whereas *Pax6* was only downregulated in TCDDHFD females compared to COChow females (**Fig. 8F**). Interestingly, *Nkx6.1* was upregulated in COHFD compared to COChow females, but expression was downregulated in TCDDHFD females compared to both COHFD and TCDDChow females (**Fig. 8E**). These results suggest that TCDD exposure may alter diet-induced changes in beta cell specific gene expression.

Lastly, the "Alanine, Aspartate and Glutamate Metabolism" pathway heatmap showed that COHFD and TCDD-exposed females formed a separate cluster compared to COChow females, suggesting that both HFD feeding and TCDD exposure alter amino acid metabolism (**Fig. 8B, Supp. Fig. 2D**). Interestingly, TCDDHFD females formed a separate subcluster compared to both TCDDChow and COHFD females, suggesting that TCDD may alter HFD-induced changes in amino acid metabolism (**Fig. 8B**).

Discussion

In this study, 12 weeks of low-dose TCDD exposure alone did not impact glucose homeostasis or plasma insulin levels in male or female mice, suggesting that background level TCDD exposure may not be sufficient to induce diabetes. TCDD exposure also did not affect the metabolic response to HFD feeding in male mice. However, when challenged with HFD feeding, TCDD exposure accelerated the onset of HFD-induced hyperglycemia in female mice by at least 4 weeks. An interaction between TCDD exposure and HFD feeding was also evident in the insulin response to a glucose challenge in females. HFD feeding induced hyperinsulinemia in CO-exposed female mice and both TCDD- and CO-exposed male mice, but failed to induce compensatory hyperinsulinemia in TCDD-exposed females. RNAseq analysis showed that TCDD exposure promoted abnormal changes to endocrine and metabolic pathways in HFD-fed females.

Our study demonstrates that the effects of chronic low-dose TCDD exposure on glucose metabolism are sex-dependent. TCDD accelerated the onset of diet-induced hyperglycemia and prevented diet-induced hyperinsulinemia, but only in female mice. There were no differences in

islet size or pancreatic endocrine cell composition to explain the discrepancy in insulin levels in TCDDHFD females. Instead, our RNAseq data points to a possible defect in beta cell function and impaired metabolic adaptability in females. For example, expression of MODY genes differed between TCDDHFD and COHFD females, indicating an interaction between TCDD and HFD on beta-cell specific genes. In fact, the diet-induced decrease in *MafA*, *Hnf4α*, and *Slc2a2* was worsened in TCDD-exposed females, whereas *Pax6* was downregulated only in TCDDHFD compared to COChow females. Further, the compensatory increase in *Nkx6.1* in COHFD females compared to COChow was absent in TCDDHFD females. These findings are in line with our previous work showing that female mice exposed to low-dose TCDD during pregnancy/lactation and subsequently fed HFD later in life had accelerated onset of hyperglycemia, transient low glucose-induced plasma insulin levels, and reduced $MafA^+$ beta cells compared to COHFD females (24). The beta cell transcription factors MAFA, PDX1, HNF4α, and PAX6 form a complex network essential for maintaining beta cell identity and regulating genes involved in insulin secretion (e.g. *Slc2a2*); inactivation of these genes is associated with beta cell dedifferentiation and metabolic inflexibility (31). Under conditions of nutrient overload, beta cells must compensate for changes in metabolic demand by altering the rate and amount of insulin secreted; failure to adapt is associated with diabetes (32). Our results suggest that low-dose TCDD exposure may promote diet-induced beta cell dedifferentiation, which could contribute to impaired metabolic adaptability and increase diabetes risk in female mice, but further research is required to support this hypothesis.

RNAseq analysis also revealed unique changes in metabolic and endocrine pathways in TCDDHFD females compared to chow-fed females that further support a defect in metabolic adaptability. We focus on two pathways of interest here, however future studies should further investigate the interactive effect of TCDD and HFD on other pathways that were enriched in our study, including “Thyroid Signalling”, “Foxo1 Signaling”, “Regulation of Actin Cytoskeleton”, amongst others. Our analysis revealed changes in the “Circadian Rhythm” pathway in islets from TCDDHFD females. Clock genes were generally altered by diet, however hierarchal clustering revealed overall differences in gene expression between CO- and TCDD-exposed females fed either a chow or HFD diet. These results suggest that both TCDD and HFD alter circadian rhythm, in line with previous data (33,34), but also that TCDD may impair normal alterations to islet circadian rhythms during HFD feeding. These data are interesting given that alterations to the circadian clock has been associated with diabetes, obesity, and metabolic syndrome in humans (35–37). Abnormal expression of clock genes has also been reported in islets from T2D donors compared to non-diabetic donors, and insulin content was positively correlated with expression of clock genes, suggesting that disruptions to the islet circadian clock may contribute to beta cell dysfunction and diabetes pathogenesis (38). In fact, knockdown of *Clock* in human islets also led to dysfunctional glucose-stimulated insulin secretion and altered the expression of genes involved in insulin secretion (39). In addition, islet-specific *Clock* knockout mice and pancreas-specific *Bmal1* knockout mice exhibit hypoinsulinemia, hyperglycemia, glucose intolerance, and an impaired insulin secretory response (40). Lastly, experimental disruption of circadian rhythms accelerates the onset of hyperglycemia and loss of functional beta cells in diabetes-prone rats (41). Taken together, our data suggest that the glucose intolerance and reduced plasma insulin levels in TCDDHFD female mice may involve altered islet circadian rhythms, but more detailed analysis is required to understand the mechanism involved.

Chronic low-dose TCDD exposure also promoted alterations to amino acid metabolism pathways in HFD-fed females. Exposure to TCDD has been previously associated with changes to circulating amino acid concentrations (42–44) and hepatic amino acid metabolism genes *in vivo* (45) and *in vitro* (46,47). Our data indicates that TCDD may also alter amino acid metabolism in islets under conditions of HFD feeding, which may have important implications for diabetes risk. Amino acids play an important role in maintaining beta cell function (48). Several studies have shown that amino acids enhance glucose-stimulated insulin secretion in islets *ex vivo* and in beta cell lines (49–51), and may indirectly regulate lipid-stimulated insulin secretion by activating enzymes involved in lipid metabolism (52,53). Amino acids have also been shown to promote the expression of genes involved in beta cell signalling, metabolism, and insulin secretion (e.g. *Pdx1*) (54,55). As such, perturbations to amino acid metabolism have been associated with T2D, obesity, and insulin resistance (56). Our data suggests that impaired amino acid metabolism in islets may contribute to the reduced plasma insulin levels and hyperglycemia observed in TCDDHFD female mice, but further investigation into amino acid metabolism and amino acid-stimulated insulin secretion following TCDD exposure is required.

Lastly, our RNAseq analysis revealed interesting changes in "Xenobiotic Metabolism by CYP450". We have previously shown that acute high-dose and chronic low-dose TCDD exposure induced *Cyp1a1* expression in islets from male mice (22,23). The present study demonstrates that *Cyp1a1* is also upregulated in female islets following low-dose TCDD exposure. We also found that HFD feeding induces *Cyp1a1* expression in islets to a similar degree as TCDD exposure, suggesting a role for *Cyp1a1* in islets beyond xenobiotic metabolism. Interestingly, we have previously shown that male *Cyp1a1/1a2* knockout mice had suppressed glucose-stimulated insulin secretion compared to wildtype controls, pointing to a non-conventional role of CYP enzymes in maintaining beta cell function (22). Furthermore, the TCDD- and HFD-induced increase in *Cyp1a1* was suppressed in TCDDHFD females, suggesting cross-talk between TCDD and HFD feeding. Given that HFD feeding increases cytokine signalling (57), we speculate that there may be an interaction between AhR and cytokine signalling pathways in this mouse model. In fact, we've previously shown that exposure of human islets to high-dose TCDD *in vitro* induced a ~26-fold increase in *Cyp1a1*, which was completely prevented when cotreated with cytokines (22). Whether this impaired *Cyp1a1* induction contributes to the metabolic phenotype observed in TCDDHFD females remains unclear.

To our knowledge this is the first study to do a head-to-head comparison of the effects of chronic low-dose TCDD exposure on diabetes risk in male and female mice. Our findings are consistent with epidemiological evidence showing that females with high serum pollutant levels have a higher risk of developing diabetes than males. However, few epidemiological studies examined sex-differences in the general population with background level of pollutant exposure, and most do not consider diet as a confounding variable when studying the association between pollutant exposure and diabetes risk. Our mouse study shows that 12 weeks of chronic low-dose TCDD alone does not cause diabetes but does increase susceptibility to diet-induced diabetes in female mice, emphasizing the need to study the interaction of pollutants with other environmental factors.

Acknowledgements
We thank Salar Farokhi Boroujeni for his technical assistance with sample analysis for this project. This research was supported by a Canadian Institutes of Health Research (CIHR) Project Grant (#PJT-2018-159590), Natural Sciences and Engineering Research Council of Canada (NSERC) Discovery Grant (RGPIN-2017-06272), the Canadian Foundation for Innovation John R. Evans Leaders Fund (#37231), and an Ontario Research Fund award. M.P.H. was supported by an Ontario Graduate Scholarship (OGS) and CIHR CGS-D award. H.B. received a NSERC Undergraduate Student Research Award (USRA) and a Carleton University Walker Summer Research Award. J.E.B. is the guarantor for this work.

Author Contributions

J.E.B. and G.M. conceived the experimental design. J.E.B., G.M., and M.P.H. wrote the manuscript. G.M., M.P.H., H.B., J.Z., S.F.B, K.R.C.R., A.W., R.G., J.K.B., C.Y., and J.E.B. were involved with acquisition, analysis, and interpretation of data. All authors contributed to manuscript revisions and approved the final version of the article.

Declaration of Interest

The authors declare no competing interests.

References

1. Saeedi P, Petersohn I, Salpea P, Malanda B, Karuranga S, Unwin N, et al. Global and regional diabetes prevalence estimates for 2019 and projections for 2030 and 2045: results from the International Diabetes Federation Diabetes Atlas, 9th edition. Diabetes Res Clin Pract. 2019;157:107843.
2. Nagao M, Asai A, Sugihara H, Oikawa S. Fat intake and the development of type 2 diabetes. Endocr J. 2015;62(7):561–72.
3. Wu Y, Ding Y, Tanaka Y, Zhang W. Risk factors contributing to type 2 diabetes and recent advances in the treatment and prevention. Int J Med Sci. 2014;11(11):1185–200.
4. Liu Z, Patil IY, Jiang T, Sancheti H, Walsh JP, Stiles BL, et al. High-fat diet induces hepatic insulin resistance and impairment of synaptic plasticity. PLoS One. 2015;10(5):e0128274.
5. Taylor KW, Novak RF, Anderson HA, Birnbaum LS, Blystone C, Devito M, et al. Evaluation of the association between persistent organic pollutants (POPs) and diabetes in epidemiological studies: a national toxicology program workshop review. Environ Heal Perspect. 2013;121(7):774–83.
6. Sun W, Clark JM, Park Y. Environmental pollutants and type 2 diabetes: a review of human studies. Toxicol Environemtnal Chem. 2017;99(9–10):1283–303.
7. Kuo CC, Moon K, Thayer KA, Navas-Acien A. Environmental chemicals and type 2 diabetes: An updated systematic review of the epidemiologic evidence. Curr Diab Rep. 2013;13(6):831–49.
8. Lee DH, Lee IK, Song K, Steffes M, Toscano W, Baker BA, et al. A strong dose-response relation between serum concentrations of persistent organic pollutants and diabetes:

results from the National Health and Examination Survey 1999-2002. Diabetes Care. 2006;29:1638–44.
9. Lee YM, Ha CM, Kim SA, Thoudam T, Yoon YR, Kim DJ, et al. Low-dose persistent organic pollutants impair insulin secretory function of pancreatic b-cells: human and in vitro evidence. Diabetes. 2017;66(10):2669–80.
10. Wang SL, Tsai PC, Yang CY, Guo YL. Increased risk of diabetes and polychlorinated biphenyls and dioxins: a 24-year follow-up study of the Yucheng cohort. Diabetes Care. 2008;31(8):1574–9.
11. Lee DH, Lee INK, Jin SH, Steffes M, Jacobs DR. Association between serum concentrations of persistent organic pollutants and insulin resistance among nondiabetic adults: Results from the National Health and Nutrition Examination Survey 1999-2002. Diabetes Care. 2007;30(3):622–8.
12. Roh E, Kwak SH, Jung HS, Cho YM, Pak YK, Park KS, et al. Serum aryl hydrocarbon receptor ligand activity is associated with insulin resistance and resulting type 2 diabetes. Acta Diabetol. 2015;52(3):489–95.
13. Michalek JE, Pavuk M. Diabetes and cancer in veterans of operation Ranch Hand after adjustment for calendar period, days of spraying, and time spent in Southeast Asia. J Occup Environ Med. 2008;50(3):330–40.
14. Consonni D, Pesatori AC, Zocchetti C, Sindaco R, D'Oro LC, Rubagotti M, et al. Mortality in a population exposed to dioxin after the Seveso, Italy, accident in 1976: 25 years of follow-up. Am J Epidemiol. 2008;167(7):847–58.
15. Vena J, Boffetta P, Becher H, Benn T, Bas Bueno-de-Mesquita H, Coggon D, et al. Exposure to dioxin and nonneoplastic mortality in the expanded IARC international cohort study of phenoxy herbicide and chlorophenol production workers and sprayers. Environ Health Perspect. 1998;106:645–53.
16. Rylander L, Rignell-Hydbom A, Hagmar L. A cross-sectional study of the association between persistent organochlorine pollutants and diabetes. Environ Heal A Glob Access Sci Source. 2005;4:28.
17. Airaksinen R, Rantakokko P, Eriksson JG, Blomstedt P, Kajantie E, Kiviranta H. Association between type 2 diabetes and exposure to persistent organic pollutants. Diabetes Care. 2011;34(9):1972–2303.
18. Glynn AW, Granath F, Aune M, Atuma S, Darnerud PO, Bjerselius R, et al. Organochlorines in Swedish women: determinants of serum concentrations. Environ Health Perspect. 2003;111:349–55.
19. Pesatori AC, Zocchetti C, Guercilena S, Consonni D, Turrini D, Bertazzi PA. Dioxin exposure and non-malignant health effects: a mortality study. Occup Environ Med. 1998;55:126–31.
20. Vasiliu O, Cameron L, Gardiner J, DeGuire P, Karmaus W. Polybrominated biphenyls, polychlorinated biphenyls, body weight, and incidence of adult-onset diabetes mellitus. Epidemiology. 2006;17:352–9.
21. IARC Working Group on the Evaluation of Carcinogenic Risks to Humans. Chemical agents and related occupations. IARC monographs on the evaluation of carcinogenic risks to humans / World Health Organization, International Agency for Research on Cancer. 2012. Volume 100F.
22. Ibrahim M, MacFarlane EM, Matteo G, Hoyeck MP, Rick KRC, Boroujeni SF, et al. Functional cytochrome P450 1a enzymes are induced in mouse and human islets

following pollutant exposure. Diabetologia. 2020;63:162–78.
23. Hoyeck MP, Blair H, Ibrahim M, Solanki S, Elsawy M, Prakash A, et al. Long-term metabolic consequences of acute dioxin exposure differ between male and female mice. Sci Rep. 2020;10(1):1448.
24. Hoyeck MP, Merhi R, Blair H, Spencer CD, Payant MA, Martin Alfonso DI, et al. Female mice exposed to low-doses of dioxin during pregnancy and lactation have increased susceptibility to diet-induced obesity and diabetes. bioRxiv. 2020;195552.
25. Angrish MM, Mets BD, Jones AD, Zacharewski TR. Dietary fat is a lipid source in 2,3,7,8-Tetrachlorodibenzo-ρ-Dioxin (TCDD)-elicited hepatic steatosis in C57BL/6 mice. Toxicol Sci. 2012;128(2):377–86.
26. R Core Team. R: A language and environment for statistical computing [Internet]. R Foundation for Statistical Computing, Vienna, Austria. 2020. Available from: https://www.r-project.org/
27. Love MI, Huber W, Anders S. Moderated estimation of fold change and dispersion for RNA-seq data with DESeq2. Genome Biol. 2014;15(550).
28. Zhu A, Ibrahim JG, Love MI. Heavy-Tailed prior distributions for sequence count data: Removing the noise and preserving large differences. Bioinformatics. 2019;35(12):2084–92.
29. Huang DW, Sherman BT, Lempicki RA. Bioinformatics enrichment tools: Paths toward the comprehensive functional analysis of large gene lists. Nucleic Acids Res. 2009;37(1):1–13.
30. Huang DW, Sherman BT, Lempicki RA. Systematic and integrative analysis of large gene lists using DAVID bioinformatics resources. Nat Protoc. 2009;4(1):44–57.
31. Bensellam M, Jonas JC, Laybutt DR. Mechanisms of β-cell dedifferentiation in diabetes: Recent findings and future research directions. J Endocrinol. 2018;236(2):R109–43.
32. Wortham M, Sander M. Mechanisms of β-cell functional adaptation to changes in workload. Diabetes, Obes Metab. 2016;18:78–86.
33. Fader KA, Nault R, Doskey CM, Fling RR, Zacharewski TR. 2,3,7,8-Tetrachlorodibenzo-p-dioxin abolishes circadian regulation of hepatic metabolic activity in mice. Sci Rep. 2019;9:6514.
34. Kohsaka A, Laposky AD, Ramsey KM, Estrada C, Joshu C, Kobayashi Y, et al. High-fat diet disrupts behavioral and molecular circadian rhythms in mice. Cell Metab. 2007;6(5):414–21.
35. Barbadoro P, Santarelli L, Croce N, Bracci M, Vincitorio D, Prospero E, et al. Rotating shift-work as an independent risk factor for overweight Italian workers: a cross-sectional study. PLoS One. 2013;8(5):e63289.
36. Scheer FAJL, Hilton MF, Mantzoros CS, Shea SA. Adverse metabolic and cardiovascular consequences of circadian misalignment. Proc Natl Acad Sci U S A. 2009;106(11):4453–8.
37. Karlsson B, Knutsson A, Lindahl B. Is there an association between shift work and having a metabolic syndrome? Results from a population based study of 27 485 people. Occup Environ Med. 2001;58(11):747–52.
38. Stamenkovic JA, Olsson AH, Nagorny CL, Malmgren S, Dekker-Nitert M, Ling C, et al. Regulation of core clock genes in human islets. Metabolism. 2012;61(7):978–85.
39. Saini C, Petrenko V, Pulimeno P, Giovannoni L, Berney T, Hebrok M, et al. A functional circadian clock is required for proper insulin secretion by human pancreatic islet cells.

Diabetes, Obes Metab. 2016;18(4):355–65.
40. Marcheva B, Ramsey KM, Buhr ED, Kobayashi Y, Su H, Ko CH, et al. Disruption of the clock components CLOCK and BMAL1 leads to hypoinsulinaemia and diabetes. Nature. 2010;466:627–31.
41. Gale JE, Cox HI, Qian J, Block GD, Colwell CS, Matveyenko A V. Disruption of circadian rhythms accelerates development of diabetes through pancreatic beta-cell loss and dysfunction. J Biol Rhythms. 2011;26(5):423–33.
42. Christian BJ, Menahan LA, Peterson RE. Intermediary metabolism of the mature rat following 2,3,7,8-tetrachlorodibenzo-p-dioxin treatment. Toxicol Appl Pharmacol. 1986;83(2):360–78.
43. Unkila M, Pohjanvirta R, Macdonald E, Tuomisto JT, Tuomisto J. Dose response and time course of alterations in tryptophan metabolism by 2,3,7,8-tetrachlorodibenzo-p-dioxin (TCDD) in the most TCDD-susceptible and the most TCDD-resistant rat strain: relationship with TCDD lethality. Toxicol Appl Pharmacol. 1994;128(2):280–92.
44. Viluksela M, Unkila M, Pohjanvirta R, Tuomisto JT, Stahl BU, Rozman KK, et al. Effects of 2,3,7,8-tetrachlorodibenzo-p-dioxin (TCDD) on liver phosphoenolpyruvate carboxykinase (PEPCK) activity, glucose homeostasis and plasma amino acid concentrations in the most TCDD-susceptible and the most TCDD-resistant rat strains. Arch Toxicol. 1999;73:323–36.
45. Boverhof DR, Burgoon LD, Tashiro C, Sharratt B, Chittim B, Harkema JR, et al. Comparative toxicogenomic analysis of the hepatotoxic effects of TCDD in Sprague Dawley rats and C57BL/6 mice. Toxicol Sci. 2006;94(2):398–416.
46. Jennen D, Ruiz-Aracama A, Magkoufopoulou C, Peijnenburg A, Lommen A, van Delft J, et al. Integrating transcriptomics and metabonomics to unravel modes-of-action of 2,3,7,8-tetrachlorodibenzo-p-dioxin (TCDD) in HepG2 cells. BMC Syst Biol. 2011;5(1):139.
47. Jennen DGJ, Magkoufopoulou C, Ketelslegers HB, van Herwijnen MHM, Kleinjans JCS, van Delft JHM. Comparison of HepG2 and HepaRG by whole-genome gene expression analysis for the purpose of chemical hazard identification. Toxicol Sci. 2010;115(1):66–79.
48. Newsholme P, Brennan L, Bender K. Amino acid metabolism, β-cell function, and diabetes. Diabetes. 2006;55:S39–49.
49. Smith PA, Sakura H, Coles B, Gummerson N, Proks P, Ashcroft FM. Electrogenic arginine transport mediates stimulus-secretion coupling in mouse pancreatic β-cells. J Physiol. 1997;499(3):625–35.
50. Brennan L, Shine A, Hewage C, Paul G Malthouse J, Brindle KM, McClenaghan N, et al. A nuclear magnetic resonance-based demonstration of substantial oxidative L-alanine metabolism and L-alanine-enhanced glucose metabolism in a clonal pancreatic β-cell line: Metabolism of L-alanine is important to the regulation of insulin secretion. Diabetes. 2002;51(6):1714–21.
51. Dixon G, Nolan J, McClenaghan N, Flatt PR, Newsholme P. A comparative study of amino acid consumption by rat islet cells and the clonal beta-cell line BRIN-BD11 - The functional significance of L-alanine. J Endocrinol. 2003;178(3):447–54.
52. Gaussin V, Hue L, Stalmans W, Bollen M. Activation of hepatic acetyl-CoA carboxylase by glutamate and Mg2+ is mediated by protein phosphatase-2A. Biochem J. 1996;316:217–24.
53. Kowluru A, Chen HQ, Modrick LM, Stefanelli C. Activation of acetyl-coa carboxylase by

a glutamate-and magnesium-sensitive protein phosphatase in the islet β-Cell. Diabetes. 2001;50(7):1580–7.
54. Cunningham GA, McClenaghan NH, Flatt PR, Newsholme P. L-alanine induces changes in metabolic and signal transduction gene expression in a clonal rat pancreatic β-cell line and protects from pro-inflammatory cytokine-induced apoptosis. Clin Sci. 2005;109(5):447–55.
55. Corless M, Kiely A, McClenaghan NH, Flatt PR, Newsholme P. Glutamine regulates expression of key transcription factor, signal transduction, metabolic gene, and protein expression in a clonal pancreatic β-cell line. J Endocrinol. 2006;190(3):719–27.
56. Adams SH. Emerging perspectives on essential amino acid metabolism in obesity and the insulin-resistant state. Adv Nutr. 2011;2(6):445–56.
57. Duan Y, Zeng L, Zheng C, Song B, Li F, Kong X, et al. Inflammatory links between high fat diets and diseases. Front Immunol. 2018;9:2649.

Figure Legends

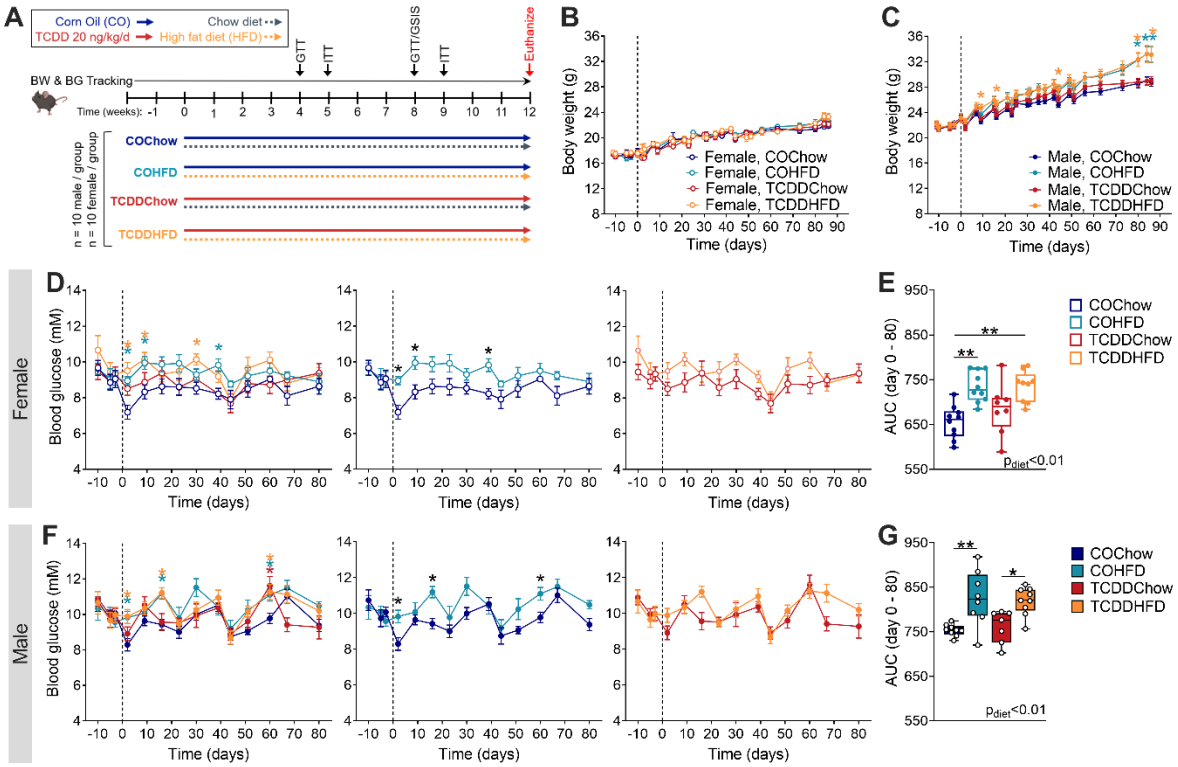

Fig. 1 Chronic low-dose TCDD exposure does not impact body weight or fasting blood glucose levels in chow-fed or HFD-fed mice. (**A**) Male and female mice were exposed to corn oil or 20 ng/kg/d TCDD 2x/week for 12 weeks, and simultaneously fed either a chow diet or a 45% HFD. Body weight and blood glucose was tracked throughout the 12 week study. BW = body weight; BG = blood glucose; GTT = glucose tolerance test; GSIS = glucose-stimulated insulin secretion; ITT = insulin tolerance test. (**B-C**) Body weight and (**D-G**) blood glucose were measured weekly following a 4-hour morning fast in (**B, D, E**) females and (**C, F, G**) males. Blood glucose data is presented as (**D, F**) all groups compared to COChow, COHFD versus COChow, TCDDHFD compared to TCDDChow, and (**E, G**) area under the curve for all groups. All data are presented as mean ± SEM in line graphs or min/max values in box and whisker plots. Individual data points on box and whisker plots represent biological replicates (different mice). *p <0.05, **p <0.01, coloured stars are versus COChow. The following statistical tests were used: (**B, C, D, F**) two-way REML-ANOVA with Tukey's multiple comparisons test; (**E, G**) two-way ANOVA with Tukey's multiple comparisons test.

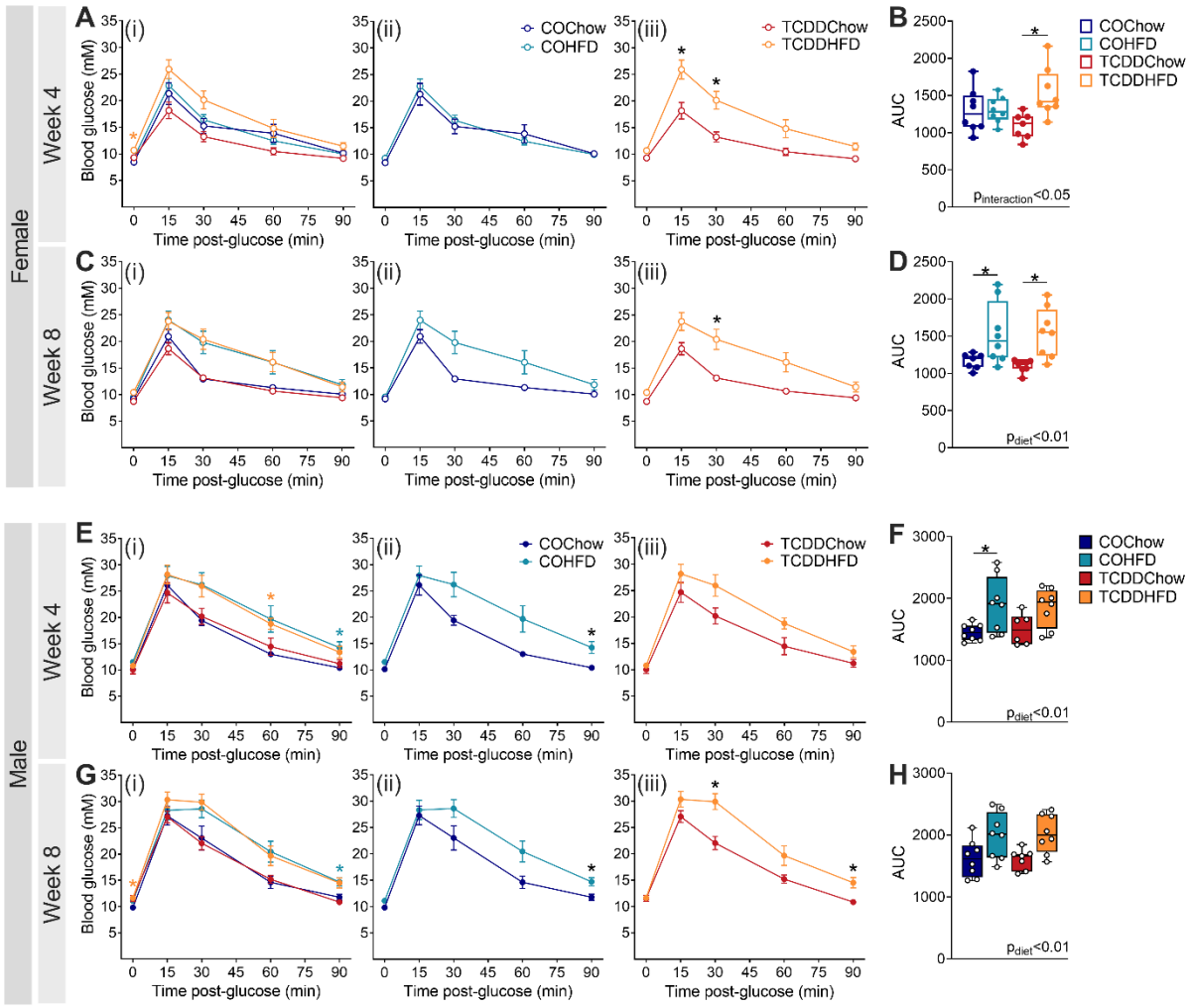

Fig. 2 TCDD exposure accelerates the onset of HFD-induced hyperglycemia in female mice. Glucose tolerance tests (GTTs) were performed after 4 and 8 weeks of TCDD exposure with/without HFD feeding (see **Fig. 1A** for study timeline). Blood glucose levels in (**A-D**) females and (**E-H**) males at week 4 (**A, B, E, F**) and 8 (**C, D, G, H**). (**A, C, E, G**) Blood glucose data is presented as (**i**) all groups compared to COChow, (**ii**) COHFD versus COChow, (**iii**) TCDDHFD compared to TCDDChow. All data are presented as mean ± SEM in line graphs or min/max values in box and whisker plots. Individual data points on box and whisker plots represent biological replicates (different mice). *p <0.05, **p <0.01. The following statistical tests were used: (**A, C, E, G**) two-way RM ANOVA with Tukey's multiple comparison test; (**B, D, F, H**) two-way ANOVA with Tukey's multiple comparison test.

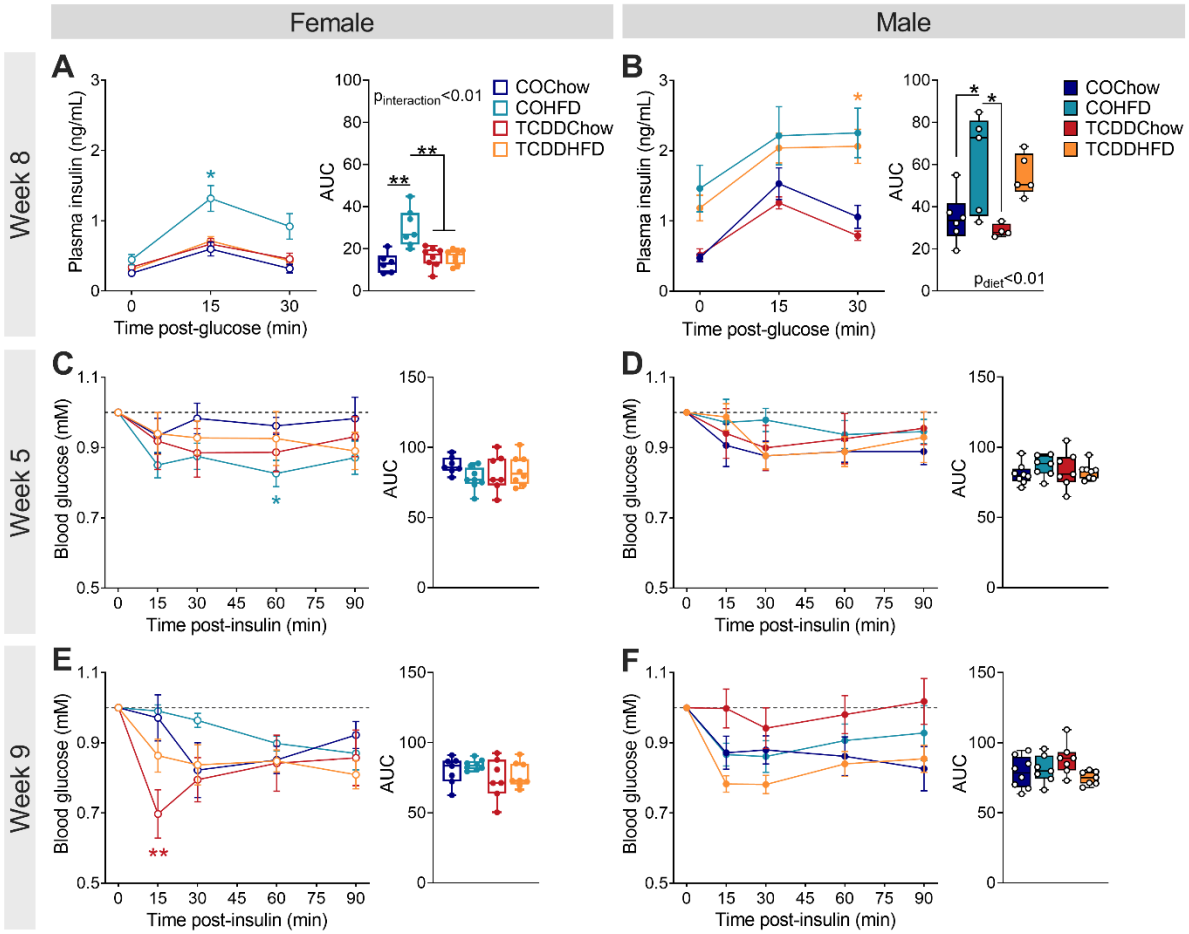

Fig. 3 TCDD-exposed female mice lack an appropriate compensatory hyperinsulinemic response to HFD feeding but had normal insulin tolerance. Glucose-stimulated insulin secretion (GSIS) was assessed *in vivo* at week 8, and insulin tolerance (ITT) at week 5 and 9 (see **Fig. 1A** for study timeline). (**A, B**) Plasma insulin levels during a GSIS at week 8 of the study in females (**A**) and males (**B**). (**C-F**) Blood glucose levels during an ITT at (**C, D**) 5 weeks and (**E, F**) 9 weeks in females (**C, E**) and males (**D, F**). All data are presented as mean ± SEM in line graphs or min/max values in box and whisker plots. Individual data points on box and whisker plots represent biological replicates (different mice). *p <0.05, **p <0.01, coloured stars are versus COChow. The following statistical tests were used: (**A-F**) line graphs, two-way RM ANOVA with Tukey's multiple comparison test; box and whisker plots, two-way ANOVA with Tukey's multiple comparison test.

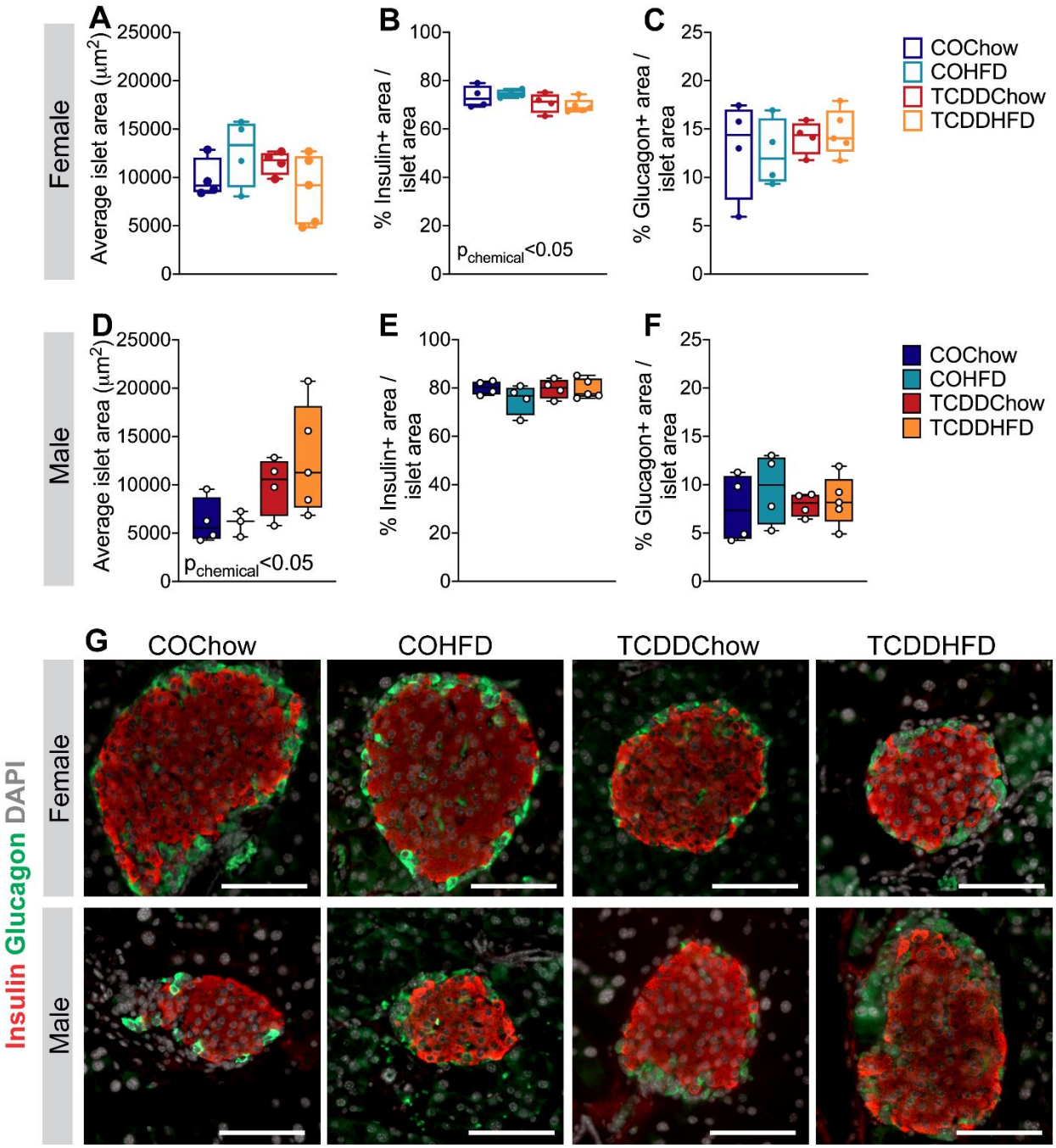

Fig. 4 Female islet size and endocrine composition were unchanged by TCDD exposure. Whole pancreas was harvested at week 12 of the study for analysis by immunofluorescence staining (see **Fig. 1A** for study timeline). (**A, D**) Average islet area, (**B, E**) % islet^{+} area / islet area, (**C, F**) % glucagon^{+} area / islet area in females (**A-C**) and males (**D-F**). (**G**) Representative images of pancreas sections showing immunofluorescence staining for insulin/glucagon. Scale bar = 100 µm. All data are presented as median with min/max values. Individual data points on box and whisker plots represent biological replicates (different mice). The following statistical tests were used: (**A-F**) two-way ANOVA with Tukey's multiple comparison test.

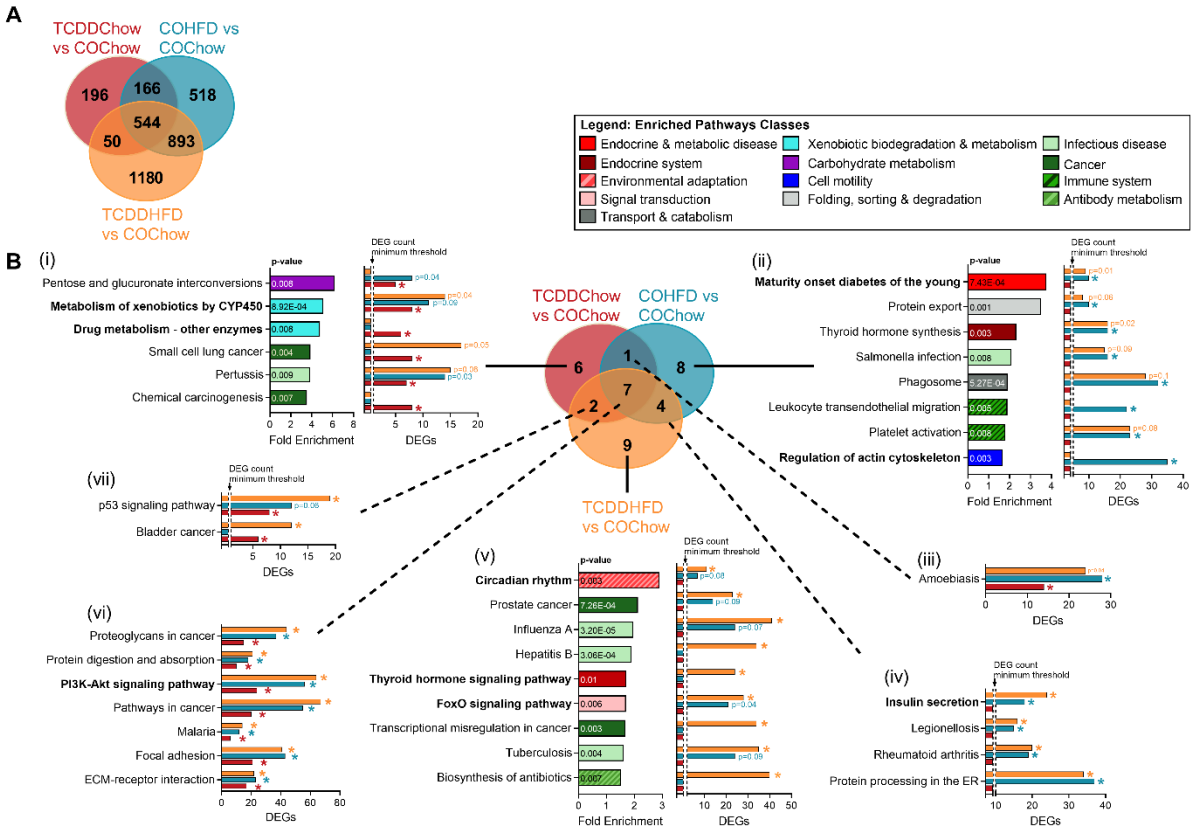

Fig. 5 TCDDHFD female mice have enriched endocrine-related pathways relative to COChow females. Islets were isolated from females at week 12 of the study for RNAseq analysis (n=3-4/group). (**A**) Venn diagram displaying differentially expressed genes (DEGs) (adjusted $p < 0.05$, absolute fold change ≥ 1.5) in all experimental groups relative to COChow females. (**B**) DAVID KEGG pathway analysis was performed on the DEGs in (**A**) for each experimental group. Results are displayed as a Venn diagram to show pathway overlap between experimental groups, as a bar graph showing pathway fold enrichment in each group relative to COChow (DAVID modified Fisher Extract p-value < 0.05 relative to COChow females), and as a bar graph comparing differentially expressed gene counts for significantly enriched pathways (coloured * = modified Fisher Extract p-value < 0.05 versus COChow).

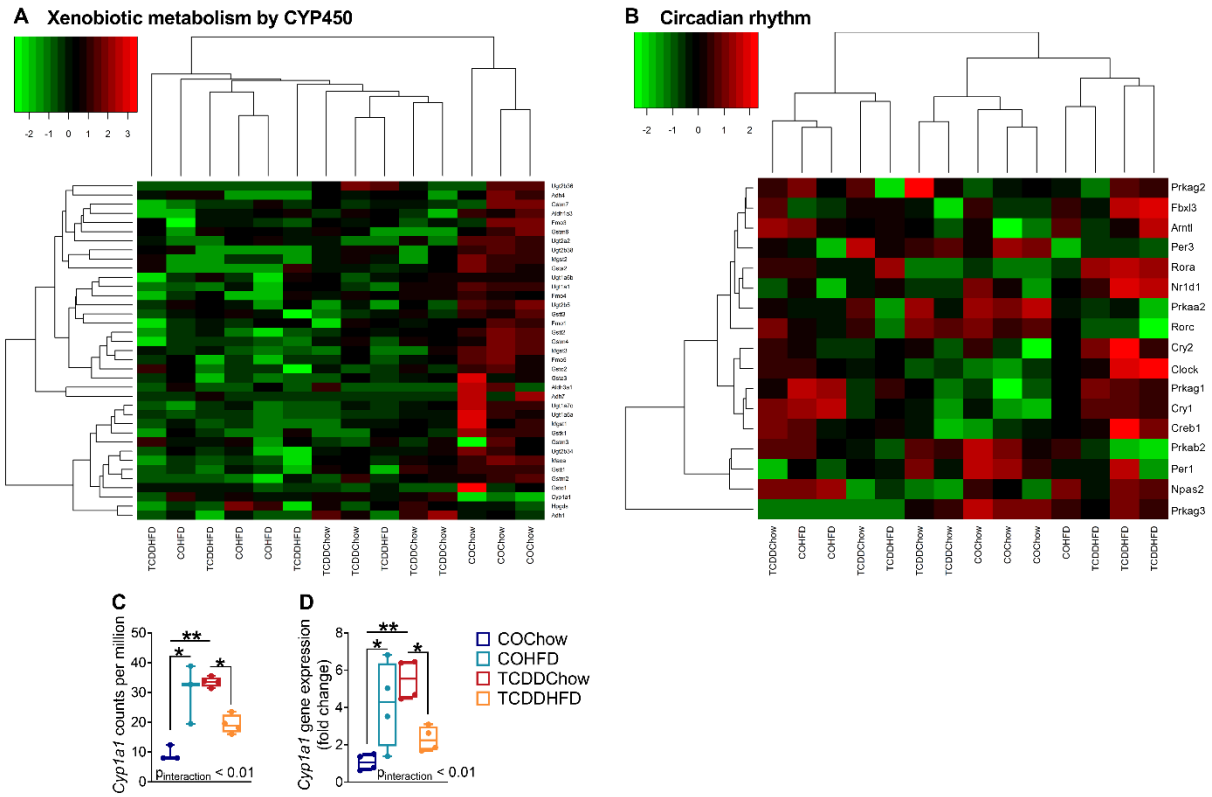

Fig. 6 TCDDHFD females have inappropriate Cyp1a1 and circadian rhythm gene expression. Islets were isolated from females at week 12 of the study for RNAseq and qPCR analysis (n=3-4/group). (**A-B**) Hierarchal heatmaps showing expression levels of gene involved in (**A**) xenobiotic metabolism by CYP450 and (**B**) circadian rhythms. (**C**) *Cyp1a1* expression in counts per million measured by RNAseq analysis. (**D**) *Cyp1a1* gene expression measured by qPCR analysis. Individual data points on box and whisker plots represent biological replicates (different mice). All data are presented as median with min/max values. *p <0.05, **p <0.01. The following statistical tests were used: (**C-D**) two-way ANOVA with Tukey's multiple comparison test.

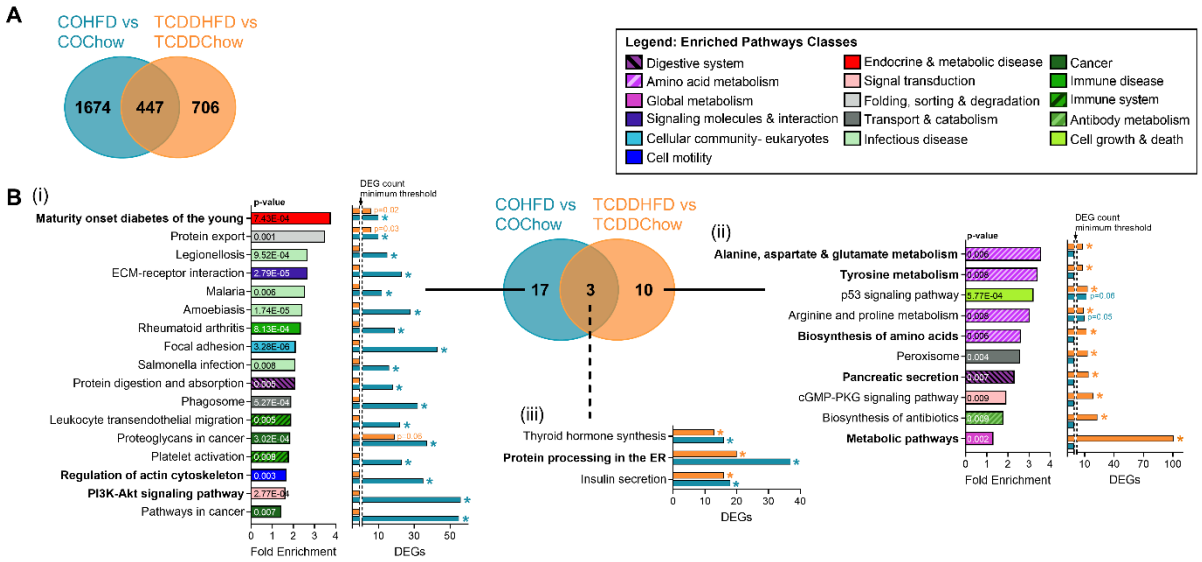

Fig. 7 Chronic low-dose TCDD exposure promotes diet-induced changes in amino acid metabolism. Islets were isolated from females at week 12 of the study for RNAseq analysis (n=3-4/group). (**A**) Venn diagram displaying differentially expressed genes (DEGs) (adjusted $p < 0.05$, absolute fold change ≥ 1.5) in HFD fed females relative their respective chow-fed control female. (**B**) DAVID KEGG pathway analysis was performed on the DEGs in (**A**). Results are displayed as a Venn diagram to show pathway overlap between experimental groups, as a bar graph showing pathway fold enrichment in each comparison (DAVID modified Fisher Extract p-value < 0.05 relative to respective chow-fed control), and as a bar graph comparing differentially expressed gene counts for significantly enriched pathways (coloured * = modified Fisher Extract p-value < 0.05 versus chow-fed control)

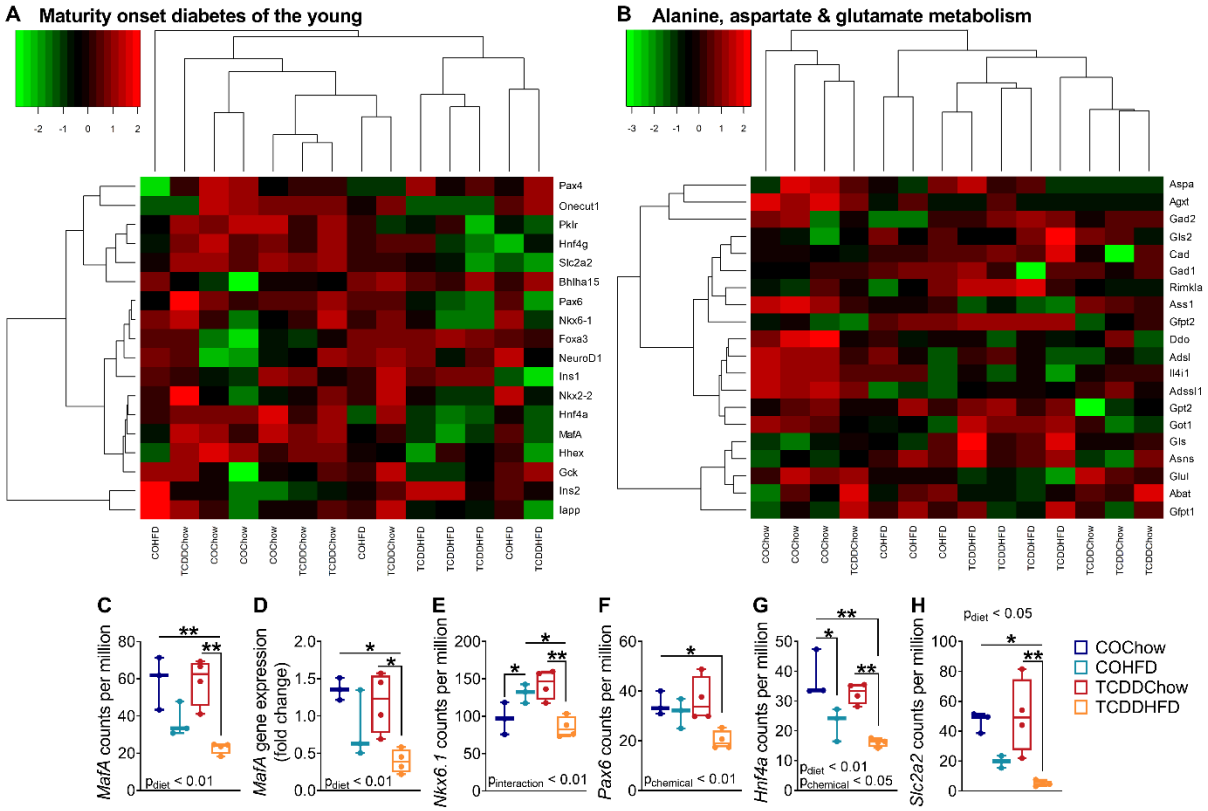

Fig. 8 HFD-induced changes in MODY genes and alanine, aspartate, and glutamate metabolism are promoted by TCDD exposure. Islets were isolated from females at week 12 of the study for RNAseq and qPCR analysis (n=3-4/group). (**A-B**) Hierarchical heatmaps showing expression levels of gene involved in (**A**) maturity onset diabetes of the young and (**B**) alanine, aspartate and glutamate metabolism. (**C, F-H**) Gene expression of (**C**) *MafA*, (**E**) *Nkx6.1*, (**F**) *Pax6*, (**G**) *Hnf4α*, and (**H**) *Slc2a2* in counts per million measured by RNAseq analysis. (**D**) *MafA* gene expression measured by qPCR analysis. Individual data points on box and whisker plots represent biological replicates (different mice). All data are presented as median with min/max values. *p <0.05, **p <0.01. The following statistical tests were used: (**C-H**) two-way ANOVA with Tukey's multiple comparison test.